Opt Quant Electron (2007) 39:491–499
DOI 10.1007/s11082-007-9083-7

Nonlinearities in the reflection and transmission spectra of the photonic bandgap heterostructures with *n–i–p–i* crystals

D. V. Ushakov · V. K. Kononenko · M. Marciniak

Received: 25 October 2006 / Accepted: 23 January 2007 / Published online: 15 June 2007

Abstract Nonlinear optical properties of photonic crystal heterostructures with embedded *n–i–p–i* superlattices are investigated. Self-consistent calculations of the transmission and reflection spectra near the defect mode are performed using the transfer-matrix method and taking into account the gain saturation. Analysis of features and output characteristics is carried out for one-dimensional photonic crystal heterostructure amplifiers in the GaAs–GaInP system having at the central part an active "defect" from doubled GaAs *n–i–p–i* crystal layers. The gain saturation in the active layers in the vicinity of the defect changes the index contrast of the photonic structure and makes worse the emission at the defect mode. Spectral bistability effect, which can be exhibited in photonic crystal heterostructure amplifiers, is predicted and the hysteresis loop and other attending phenomena are described. The bistability behavior and modulation response efficiency demonstrate the potential possibilities of the photonic crystal heterostructures with *n–i–p–i* layers as high-speed optical amplifiers and switches.

Keywords Amplifier · Gain saturation · Photonic crystal heterostructure · Spectral bistability · Transmission spectrum

PACS numbers: 05.45.Pq · 42.55.Px · 42.65.Sf

D. V. Ushakov
Belarussian State University, Independence Ave., 4, 220030 Minsk, Belarus

V. K. Kononenko (✉)
Stepanov Institute of Physics, National Academy of Science of Belarus, Independence Ave., 70, 220072 Minsk, Belarus
e-mail: lavik@dragon.bas-net.by

M. Marciniak
National Institute of Telecommunications, Szachowa Str., 1, 04-894 Warsaw, Poland

1 Introduction

Low-dimensional photonic structures are recognized at present as a natural foundation of the future high-capacity network components. In particular, the photonic band gap (PBG) structures seem promising for providing the increase of optical nonlinear response of a material in order to attain high efficiency of optical processes at rather small volume. Based on photonic crystals, different novel compact optical devices are realized, including optical switches, single-mode lasers and amplifiers, light pulse compressors, and frequency converters. A powerful principle that could be explored to implement all-optical transistors, switches, logical gates, and memory elements is the conception of optical bistability. In systems with the optical bistability the outgoing light intensity depends not only on the instantaneous input intensity but and also on the history in a hysteresis loop manner (Soljačić et al. 2002). Some of practically effective PBG structures in near-infrared (IR) and visible wavelength ranges are recently demonstrated (Lee and Yao 2003).

As a candidate for the active medium with large optical nonlinearities, *n–i–p–i* crystals or doping superlattices can be used (Ando et al. 1989; Döhler 1990). The nonlinear processes in the *n–i–p–i* superlattices are connected with (a) the filling or emptying of the energy states under optical excitation of the crystal, (b) redistribution of the energy levels at changing the potential relief depth, (c) the shortening of the density state tails, which are related to the impurity concentration fluctuations, at the screening of the electrostatic potential by non-equilibrium current carriers, (d) change in the lifetime of current carriers due to changes in the overlap of the envelope wave functions of electrons and holes, (e) masking behavior of the free carrier absorption, (f) stabilizing action of the background screening, (g) saturation of absorption or amplification, and (h) effects of narrowing the semiconductor band gap and of changing the effective band gap of the superlattice (Kononenko et al. 1998; Ushakov et al. 1999, 2001).

Doping superlattices are feasible for integration in optical circuits and, moreover, a photonic crystal heterostructure (PCH) can be fabricated in a desirable manner to provide appropriate dispersion properties and optical spectra. In previous work (Nefedov et al. 2002) we studied the possibilities to use *n–i–p–i* superlattices as optically controllable active layers in the GaAs–AlGaAs PBG structures. New types of laser microcavities based on δ-doped superlattices for providing the low-threshold lasing at multiple wavelengths and emission in opposite directions have been also examined (Smirnov et al. 2002). Different PCHs composed of doping superlattices and wide-band-gap semiconductor layers are proposed and optimized (Kononenko et al. 2003). In particular, laser sources, optical amplifiers, and switches are designed in the GaAs–GaInP system for the near-IR region. Proposed PCH elements are well provided with the Al-free technology.

In the present work, we submit results of numerical calculations and analysis of performance of PCH amplifiers in the GaAs–GaInP system lattice-matched to the GaAs substrate. Active layers are made of the GaAs *n–i–p–i* crystals with δ-doped *n*- and *p*-layers and their optical properties are controlled using electric or optical excitation. We describe two essential nonlinear effects in the PCH amplifiers with active *n–i–p–i* layers. The first one results from the appearance of two neighboring and distinct resonance peaks in the output power at the defect mode resonance depending on the excitation level and input light power. Another nonlinear effect is the bistability in the transmission and reflection spectra near the defect mode. Thus, at the defect mode of the PCHs with active *n–i–p–i* layers the bistable switching of the reflection and transmission spectra can be efficiently performed.

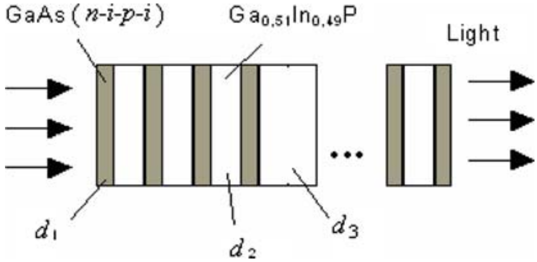

Fig. 1 Schematic design of 1D PCHs with the GaAs *n–i–p–i* crystal active layers. d_1 is the thickness of the GaAs superlattice, d_2 is the thickness of the GaInP passive layer component, d_3 is the thickness of the defect layer

The paper is organized as follows. In Sect. 2, design of the examined PCH amplifiers is shortly described. Optical properties of the PCHs, including features of transmission and reflection spectra and their nonlinear behavior, are discussed in Sect. 3 having four subsections. Special attention in Subsect. 3.2 is given gain saturation processes. Final conclusions are presented in Sect. 4.

2 Photonic component design

For constructing a compositional PBG material we suggest to use heterostructures in the GaAs–$Ga_xIn_{1-x}P$ system, which are lattice-matched to the GaAs substrate (Fig. 1). Each layer is characterized by the thickness d and complex refractive index $n(\lambda) = n_r(\lambda) - i\kappa(\lambda)$. Active layers are made as the GaAs *n–i–p–i* crystals with δ-doped n- and p-layers of 2.8 nm-thickness and $5.3\times10^{19}cm^{-3}$-donor and acceptor concentrations and with i-layers of 11.3 nm-thickness. The superlattice period is markedly smaller than the period of the PCH, therefore the approximation of the effective refractive index is applied for the description of the active medium optical properties. The refractive index n_r and coefficient of extinction κ of *n–i–p–i* superlattice layers depends on the light wavelength λ and difference in the quasi-Fermi levels ΔF (Ushakov et al. 2001).

We consider the case, where the active layers of the PCH amplifier are uniformly excited by the electric or optical manner. Detail analysis of the output power performance and occurring nonlinear effects is carried out for one-dimensional (1D) PCH amplifiers having at the central part an active "defect" from the doubled GaAs *n–i–p–i* crystal. Light is assumed propagating perpendicularly to the interfaces of layers.

In general, composition of PCHs can be presented as $(AB)D(AB)$ where A is an active material, B is a passive material, and D is a defect (Smirnov et al. 2002). The passive component layers are 72.3 nm-thickness layers of a wide-gap semiconductor $Ga_xIn_{1-x}P$ with the mole fraction $x = 0.51$ and energy band gap of 1.89 eV. In the PCH amplifier under general consideration, a doubled superlattice at the center offers an active defect component D and the defect mode occurs near the wavelength of 0.95 μm, while the PBG covers a range of 0.93–0.97 μm.

The input power P_{in} is assumed to be up to 400 W/cm^2. Since the gain saturation, the quantities of ΔF and refractive index n are changed from layer to layer and in the layers. The maximum variations occur in the vicinity of the defect layer (Kononenko et al. 2004). In general, the light field distribution in the PCHs is noticeably affected by dispersion parameters of the components and by conditions at the end faces.

3 Optical properties of photonic heterostructures

3.1 Background of calculations

The self-consistent calculations of the transmission and reflection spectra have been performed using the transfer-matrix method and taking into account the saturation effects. The transfer matrix across layer j in a PCH can be expressed as (Born and Wolf 1999)

$$G_j = \begin{pmatrix} \cos \xi_j & -i/n_j \sin \xi_j \\ -in_j \sin \xi_j & \cos \xi_j \end{pmatrix}, \tag{1}$$

where $\xi_j = (2\pi \nu/c)\, d_j n_j$, n_j is the complex refractive index, d_j is the thickness of the j-layer, ν is the wave frequency. Thus, a transfer matrix across a structure composed by N layers is found in the form

$$M = \prod_{j=1}^{N} G_j. \tag{2}$$

Matrix M connects tangential electromagnetic field components E_i, E_r at the input $z = 0$ and E_t at the output $z = L$ of the PCH, i.e.,

$$\begin{pmatrix} A_0 \\ B_0 \end{pmatrix} = M \begin{pmatrix} A_L \\ B_L \end{pmatrix}. \tag{3}$$

Here, $A_0 = E_\mathrm{i} + E_\mathrm{r}$, $B_0 = E_\mathrm{i} - E_\mathrm{r}$, $A_L = E_\mathrm{t}$, $B_L = E_\mathrm{t}$, and the amplitude and power transmission (t, T) and reflection (r, R) coefficients are determined as $t = E_t/E_i$, $T = |t|^2$, $r = E_r/E_i$, $R = |r|^2$. The input power P_{in} is defined by the formula

$$P_\mathrm{in} = v_\mathrm{g} U = \frac{c\varepsilon_0 |E_i|^2}{2}, \tag{4}$$

where v_g is the group velocity of light, U is the density of energy of monochromatic electromagnetic wave.

Quantitative description of the gain saturation and accompanying nonlinear refraction effects is carried out for 1D PCH amplifiers having at the central part an active defect component from the doubled GaAs *n–i–p–i* crystal. Here, the nonlinear gain spectrum is calculated for δ-doped layer superlattices and changes in the refractive index within the PBG of the PCH amplifiers are determined.

3.2 Gain saturation process

For the determining of the dependence of the gain coefficient on the density of energy of the electromagnetic field in every active *n–i–p–i* layer, the standard system of the stationary rate equations for non-equilibrium current carriers in the quantum wells of the superlattice potential relief and the photon density is used (Kononenko and Gribkovskii 1970; Ushakov 2001). The rate of generation (excitation) of current carriers is determined by the initial value of the quasi-Fermi difference ΔF_0 if the nonlinear effects are not essential and the radiation flux is negligible. The definite rate of spontaneous radiative recombination R_{sp0} corresponds to this value ΔF_0. In general case, the gain coefficient $k(\nu)$ in the active layers is related to the sum rate of radiative and non-radiative recombination R_{sp}/η_{sp} in a separate active layer and to the density of energy U of monochromatic electromagnetic wave propagating in the PCH according to the expression

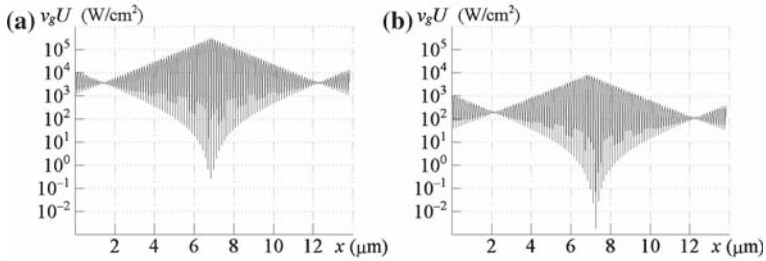

Fig. 2 Spatial distribution of the radiation intensity $v_g U(x)$ in the PCH at the defect mode wavelength λ_0 under different excitations of the active *n–i–p–i* layers (**a**) $\Delta F_0 = 1.41$ and (**b**) 1.44 eV, the input radiation power $P_{in} = 10\,\mathrm{W/cm^2}$

$$k(\nu) = \frac{h\nu}{v_g U}\left(\frac{R_{\mathrm{sp0}}}{\eta_{\mathrm{sp0}}} - \frac{R_{\mathrm{sp}}}{\eta_{\mathrm{sp}}}\right). \tag{5}$$

Here $h\nu$ is the photon energy, η_{sp} is the quantum yield of luminescence, The non-radiative recombination lifetime constant can be in particular taken equaled to $\tau_{nr} = 1\mu$s.

The gain saturation effect is associated with the approaching of the quasi-Fermi level difference ΔF to the photon energy $h\nu$ at increasing the monochromatic radiation intensity. At sufficiently high U, the gain coefficient is inverse proportional to the light flux. Then, introducing the initial gain coefficient k_0, we obtain $k = k_0/\alpha_\infty U$, where the nonlinearity parameter $\alpha_\infty = v_g k_0/h\nu(R_{sp0}/\eta_{sp0} - R_{sp}/\eta_{sp})$. Here R_{sp} corresponds to $\Delta F \approx h\nu < \Delta F_0$. In general case, the gain saturation is described by the law $k = k_0/(1 + \alpha U)$, where $\alpha \leq \alpha_\infty$. Features of nonlinear gain in injection lasers are established by analogous way (Kononenko and Gribkovskii 1970).

The nonlinearity parameter α in dependence on the radiation density in active $n-i-p-i$ layers can be of different values. At low light fluxes, $\alpha = \alpha_0$ and the gain saturation follows to the expression $k = k_0(1 - \alpha_0 U)$. For middle values of the radiation density U, where k drops at two times, it is necessary to use the quantity $\alpha = \alpha_{1/2}$. At high U, the nonlinearity parameter is $\alpha = \alpha_\infty$. Herewith, the relation $\alpha_0 < \alpha_{1/2} < \alpha_\infty$ is fulfillment. The nonlinearity parameter α decreases monotonically with the radiation wavelength λ and at the twofold drop of the gain coefficient with the increasing of U the corresponding value $\alpha_{1/2}/v_g$ at the wavelength near 0.95 μm is in the order of $1.6\times10^{-6}\,\mathrm{cm^2/W}$. (Kononenko et al. 2004).

The saturation effects are mainly associated with the potential profile transformation in the superlattice layers at increasing the monochromatic radiation intensity and have principal influence on the spatial distribution of the electromagnetic field and respectively on the operating characteristics. The gain saturation in the active layers in the vicinity of the defect changes the index contrast of the PCH. It is attributed to the changes in the spatial distribution of the refractive index due to the nonlinear refraction. Symmetry in the distribution of the electromagnetic field is broken and a bundle near the input end face penetrates into the PCH volume (Fig. 2). So, changes in the index contrast of PCHs due to the gain saturation in the central defect amplifying layers makes worse the emission at the defect mode.

3.3 Features of transmission and reflection spectra

Two new nonlinear optical effects in the PCHs with active *n–i–p–i* layers are predicted (Ushakov et al. 2003). One effect is related with the appearing of two neighboring resonance peaks of the output power in both reflection and transmission operation at the defect mode versus

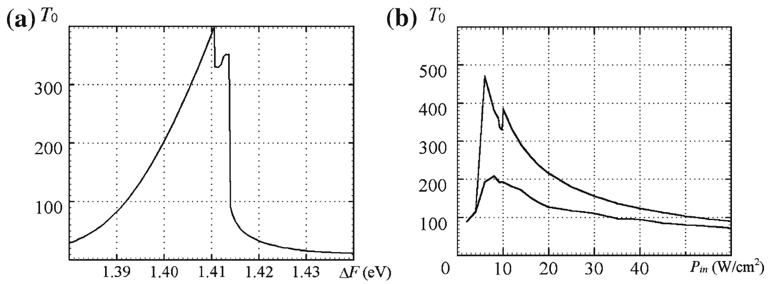

Fig. 3 Transmission coefficient T_0 of the PCH with *n–i–p–i* active layers corresponding to the maximum wavelength λ_0 of the spectrum versus (**a**) the quasi-Fermi level difference $\Delta F = \Delta F_0$, $P_{in} = 10\,\text{W/cm}^2$, and (**b**) the input power P_{in}, $\Delta F_0 = 1.41\,\text{eV}$

the pump level of the *n–i–p–i* layers (Fig. 3(a)). The pump level of the active component layers is characterized by the initial value of the quasi-Fermi level difference $\Delta F = \Delta F_0$ at electric or optical mode of excitation. Similar behavior is obtained in dependence on the input radiation power P_{in} (Fig. 3(b)).

Similar resonances appear for the dependences of the reflection coefficient R_0. The maximum wavelength λ_0 of the transmission and reflection spectra shifts to the short-wavelength region with increasing ΔF. Near $\Delta F = 1.41\,\text{eV}$ two subsequent drops of λ_0 occur. As a result, two peaks in the dependencies $T_0(\Delta F)$ and $R_0(\Delta F)$ appear. The highest values of the transmission T_0 and reflection R_0 coefficients reach up to 400 at $P_{in} = 10\,\text{W/cm}^2$. The response at the defect mode decreases with further increasing the input power P_{in}.

Another effect is bistable switching in the transmission and reflection at the spectral tuning within the defect mode band. The tuning can be realized with increasing or decreasing the signal wavelength λ. The responses in these regimes differ that reflects as a hysteresis. The width of the spectral hysteresis loop depends on the input signal intensity and pump of the nonlinear PCH.

The hysteresis character is clearly seen in Fig. 3(b) where the overhead curve is obtained for the increasing of λ and two adjacent maxima of the maximum transmission coefficient T_0 versus the input radiation power P_{in} are observed. In this regime the highest value of the transmission coefficient T_0 is 460 at the input power $P_{in} = 6\,\text{W/cm}^2$. The bottom curve in Fig. 3(b) corresponds to the maximum value of T_0 at the return spectral tuning, i.e., in the regime of the decreasing of λ.

3.4 Spectral bistability and hysteresis behavior

The bistability in the transmission and reflection spectra is pronounced near the defect mode. Changes in the refractive index, which result from the gain saturation, are responsible for respective changes in the PCH transmission spectrum. In general, a positive (negative) nonlinearity has a tendency to shift respectively the entire transmission spectrum to the left (right). Specially, when the resonance is sharp enough, bistability or multistability can be achieved (Agranovich et al. 1991). For a pure periodic structure, the bistability usually occurs near the resonance peak at the border of the PBG.

As an example, we display in Fig. 4 the transmission spectra of the PCH with active *n–i–p–i* layers in the vicinity of the defect resonance peak located in the basic PBG. Each spectrum is calculated using a fixed input power P_{in} or quasi-Fermi level difference ΔF_0. At a certain threshold P_{in} or ΔF_0 the spectrum exhibits the spectral bistability phenomenon.

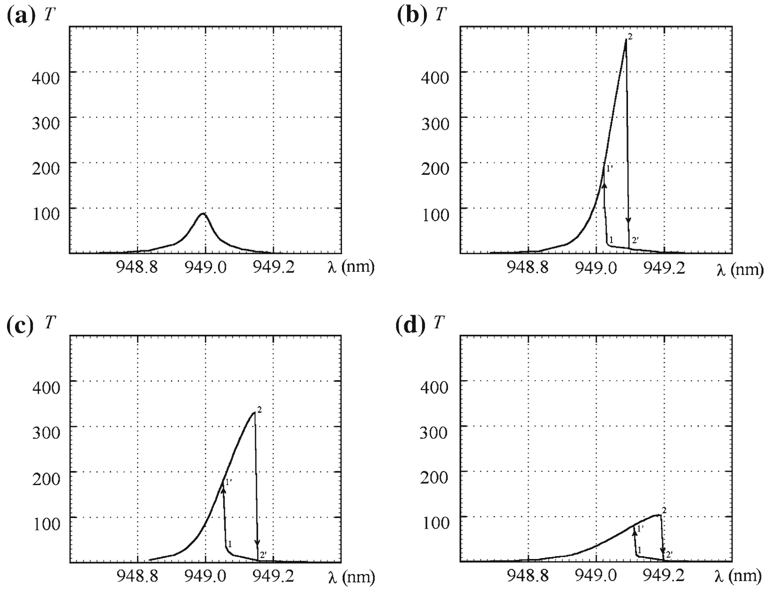

Fig. 4 Hysteresis of the transmission spectra $T(\lambda)$ in the defect mode bandwidth at different values of the input power (**a**) $P_{in} = 2$, (**b**) 6, (**c**) 12, and (**d**) 50 W/cm^2. $\Delta F_0 = 1.41\,\text{eV}$

Decreasing the wavelength of a tunable source results in the transmission jump into high-transmission state $1'$ after passing point 1. Similarly, the low-transmission state $2'$ can be reached after passing state 2 when moving in the opposite spectral direction.

Transformation of the transmission spectrum hysteresis curves with growth of an input power is also seen in Fig. 4. At small values of an input power less than 4 W/cm^2 the spectral hysteresis in the defect mode region is not manifested. In this case, both curves $T_0(P_{in})$ coincide and the hysteresis at the tuning of λ is not observed (Fig. 4(a)). At high powers both curves approach asymptotically to each other (Fig. 3(b)) and the hysteresis loop becomes less pronounced.

Changes in the reflection spectrum $R(\lambda)$ of the PCH in dependence on the input power P_{in} are similar. The amplitude of the defect mode follows non-monotonically with the input radiation intensity and is also determined by the course of tuning the wavelength (increasing or decreasing λ near the defect mode). For the curves corresponding to the increasing of λ, in the reflection operation two adjacent maxima of $R(\lambda) \approx 500$ are observed at $P_{in} = 6$ and 10 W/cm^2 (Kononenko et al. 2005).

Switching behavior in transmission mode of operation at a fixed wavelength of input light intensity is demonstrated in Fig. 5. Output–input characteristics of specific S-type appear only in a narrow spectral interval near the defect mode. This interval overlaps only 0.2 nm that is related to the PCH design and is obviously determined by the number of periods of photonic structure (Tsai et al. 1998).

The output–input characteristics of the PCH depend on the tuning of the signal wavelength out the defect mode. When the input power P_{in} increases up to a switching threshold value, the output power P_{out} jumps to a higher value (from state 1 to state $1'$). Then, P_{out} increases monotonously versus the value of P_{in}. On the other hand, when P_{in} decreases from the value that is greater than the threshold value, P_{out} decreases slowly until it reaches state 2 at which it

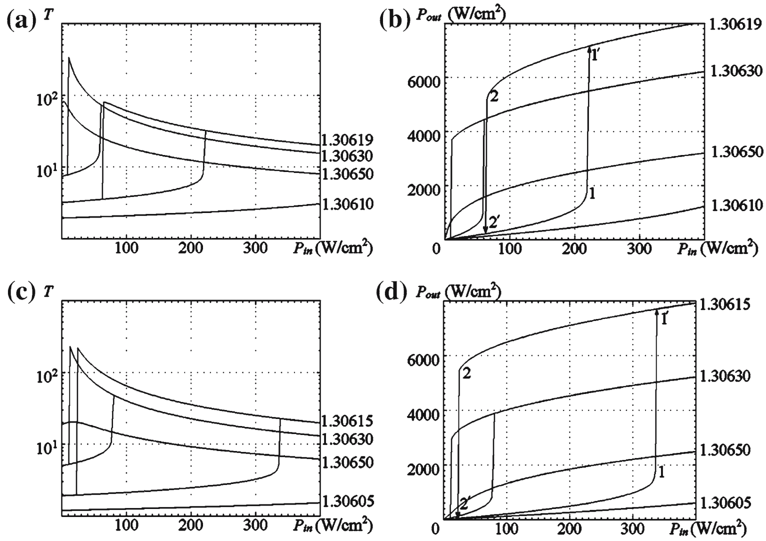

Fig. 5 Transmission–input $T(P_{in})$ and output–input $P_{out}(P_{in})$ characteristics of PCHs with structures (**a**), (**b**) $(AB)_{50}D(AB)_{50}$ and (**c**), (**d**) $(AB)_{50}D_2(AB)_{50}$ at different photon energies $h\nu$ (values on the curves in eV), $\Delta F_0 = 1.41\,\text{eV}$

jumps to state 2′. Then, P_{out} continues to decrease monotonously with the decreasing of P_{in}. It is clearly seen that the hysteresis loop width depends markedly on the signal wavelength detuning.

It should be noticed that the region between the low-output state and high-output state, i.e., lines 1–1′ and 2–2′ correspond to unstable conditions. For the PCH $(AB)_{50}D(AB)_{50}$ with single defect layer the higher switching threshold value (220 W/cm^2) and respectively larger the hysteresis loop width is observed at the defect resonance energy $h\nu = 1.30619\,\text{eV}$ (Fig. 5(b)). The detuning of the frequency (wavelength) of the input signal can reduce the switching threshold value. For example, the switching threshold at $h\nu = 1.30630\,\text{eV}$ is 60 W/cm^2. However, the bistable behavior is not obtained if the input signal wavelength is not close to the defect mode. Increasing of the defect layer number results in larger switching power threshold values and wider hysteresis loop (Fig. 5(d)).

4 Conclusion

Different PCHs composed of doping superlattices and wide-band-gap semiconductor layers are designed. Proposed in the GaAs–GaInP system laser sources, optical amplifiers, and switches are attractive for the near-IR region. The self-consistent simulation of optical properties is carried out for 1D PCH amplifiers having at the central part an active defect from the doubled GaAs *n–i–p–i* crystal. As shown, the nonlinear effects, which are mainly associated with the potential profile transformation in the superlattice layers at increasing the monochromatic radiation intensity, have principal influence on the spatial distribution of the electromagnetic field and respectively on the PCH operating characteristics.

Two new nonlinear optical effects in the PCHs with active *n–i–p–i* layers are predicted. One effect is related with the appearing of two neighboring resonance peaks of the output power in both reflection and transmission operation at the defect mode versus the pump level of the *n–i–p–i* layers. Another effect is bistable switching in the transmission and reflection at the spectral tuning within the defect mode bandwidth. The width of the spectral hysteresis loop depends markedly on the input signal intensity and on the active layer pump. Obtained data show potential opportunities of the PCHs with active *n–i–p–i* layers as high-speed optical amplifiers and switches.

References

Agranovich, V.M., Kiselev, S.A., Mills, D.L.: Optical multistability in nonlinear superlattices with very thinlayers. Phys. Rev. B **44**, 10917–10920 (1991)

Ando, H., Iwamura, H., Oohashi, H., Kanbe, H.: Nonlinear absorption in *n–i–p–i* MQW structures. IEEE J. Quantum Electron. **25**, 2135–2141 (1989)

Born, M., Wolf, E.: Principles of Optics. University Press, Cambridge (1999)

Döhler, G.H.: Non-linear optical properties of *n–i–p–i* and hetero *n–i–p–i* structures and their potential for applications in photonics. Opt. Quantum Electron. **22**, S121–S140 (1990)

Kononenko, V.K., Gribkovskii, V.P.: Effect of saturation in semiconductor light amplifiers and filters. Opt. Spectrosc. **29**, 975–984 (1970)

Kononenko, V.K., Manak, I.S., Ushakov, D.V.: Optoelectronic properties and characteristics of doping superlattices. Proc. SPIE **3580**, 10–27 (1998)

Kononenko, V.K., Marciniak, M., Ushakov, D.V.: Nonlinear gain and bistability in photonic crystal heterostructures with compositional and doping superlattices. Proc. SPIE **5950**, 56–65 (2005)

Kononenko, V.K., Smirnov, A.G., Ushakov, D.V.: Influence of gain saturation on output power characteristics of the photonic crystal type heterostructures. Bull. RAS **68**, 127–130 (2004)

Kononenko, V.K., Ushakov, D.V., Smirnov, A.G.: Photonic crystal heterostructures with controllable active layers. Proc. ICTON **1**, 247–251 (2003)

Lee, H.-Y., Yao, T.: Design and evaluation of omnidirectional one-dimensional photonic crystals. J. Appl. Phys. **93**, 819–830 (2003)

Nefedov, I.S., Gusyatnikov, V.N., Marciniak, M., Kononenko, V.K., Ushakov, D.V.: Optical gain in onedimensional photonic band gap structures with *n–i–p–i* crystal layers. J. Telecommun. Inform. Technol. 1, 60–64 (2002)

Smirnov, A.G., Ushakov, D.V., Kononenko, V.K.: Multiple-wavelength lasing in one-dimensional bandgap structures: implementation with active *n–i–p–i* layers. J. Opt. Soc. Am. B **19**, 2208–2214 (2002)

Soljačić, M., Ibanescu, M., Johnson, S.G., Fink, Y., Joannopoulos, J.D.: Optimal bistable switching in nonlinear photonic crystals. Phys. Rev. E **66**, 055601-1 (R)–055601-4 (R) (2002)

Tsai, Y.-C., Shung, K.W.-K., Gou, S.-C.: Impurity modes in one-dimensional photonic crystals-analytic approach. J. Mod. Opt. **45**, 2147–2157 (1998)

Ushakov, D.V., Kononenko, V.K., Manak, I.S.: Effects of energy spectrum broadening in doping semiconductor superlattices. J. Appl. Spectrosc. **66**, 820–825 (1999)

Ushakov, D.V., Kononenko, V.K., Manak, I.S.: Nonlinear optical properties in semiconductor doping superlattices. J. Appl. Spectrosc. **68**, 656–662 (2001)

Ushakov, D.V., Kononenko, V.K., Marciniak, M.: Nonlinear optical effects in one-dimensional photonic crystal heterostructure amplifiers. Proc. ICTON **1**, 330–332 (2003)